# Satellite Launcher Pointing for Orbit Injection with Uncontrolled Solid-Propellant Last Stage

*Abel de Lima Nepomuceno* and Waldemar de Castro Leite Filho***
**Instituto de Aeronáutica e Espaço*
*Praça Eduardo Gomes, 50 , 12228-904 Sao José dos Campos-SP, Brasil*
*** Instituto de Aeronáutica e Espaço*
*Praça Eduardo Gomes, 50 , 12228-904 Sao José dos Campos-SP, Brasil*

## Abstract
An orbit injection method is proposed for satellite launchers with uncontrolled last stage, addressing both orbit plane geometry and inclination issues. An impulsive approach is used to model the transferring to orbit, with last stage burning synchronized through its thrust acceleration profile. The method is also supported on strong in-flight identification of suborbital trajectory parameters, and feasibility pre-evaluation within fault conditions and requirements priorities. Then, an iterative procedure determines, to the chosen precision, the parameters values needed to proceed the orbit injection. Simulation tests results allow testifying the good performance and reliability of the method.

## 1. Introduction

After the initial propelled ascending phases and already beyond atmosphere, the considered launcher vehicle goes on a Keplerian suborbital trajectory phase, with attitude control capability. Along this suborbital trajectory, the vehicle should be positioned and stabilized in an adequate inertial longitudinal angular attitude to, at an adequate time, start the transferring into satellite final orbit, through the propulsion of an uncontrolled (no control on thrust intensity and direction) last stage. The satellite orbit is required to have a given inclination and a given eccentricity. An on-board pointing algorithm is in charge of providing the values of those adequate vehicle longitudinal attitude and last stage start-up time, so that the satellite is injected into an orbit with the required inclination and eccentricity.
The method presented here is a pointing algorithm based on the concept of impulsive orbit transfer [1], where there are the parameters impulsive transfer ray, or impulse ray, and impulsive transfer time, or impulse time. This impulse ray becomes the orbit injection ray; and this impulse time becomes a reference to fix the last stage start-up time. It is considered that the orbit transfer is to be done by the target orbit perigee. Locally, the vehicle longitudinal attitude is specified by a local pitch angle and a local yaw angle. There is a proceeding to calculate the impulse ray, local pitch angle and timing, using a fixed value of the local yaw angle. There is another proceeding to calculate the local yaw angle and recalculate the local pitch angle, using a fixed value of the impulse ray. Hence, these proceedings are executed alternately and iteratively, till calculated values converge, following the chosen convergence criteria. By construction of the method, there is convergence in any situation, with a low limit in the number of iterations.

## 2. Pointing method development

### 2.1 Orbit transfer synchronizing

The impulsive orbit transfer is associated to an impulse time $t_i$, at which the transfer would occur. But the time interval $\tau$, of propulsion during transfer, is finite. Therefore, the time $t_0$, at which the propulsion should start, must be determined. We consider the following data about the solid-propellant last stage used for the orbit transfer:
$\tau$ : time interval of propulsion.
$mc$ : Total mass of components (excluding propellant).
$mp(t)$ , $0 \le t \le \tau$ : Time-varying propellant mass profile.
$T(t)$ , $0 \le t \le \tau$ : Time-varying vacuum thrust profile.
$Ap(t)$ , $0 \le t \le \tau$ : Time-varying propulsion acceleration profile.
$\Delta Vp = \|\mathbf{\Delta Vp}\|$ : Speed increment, or characteristic speed, due to propulsion.

Figure 1 illustrates the orbit transfer. Some symbols in the figure are defined in the subsections below.

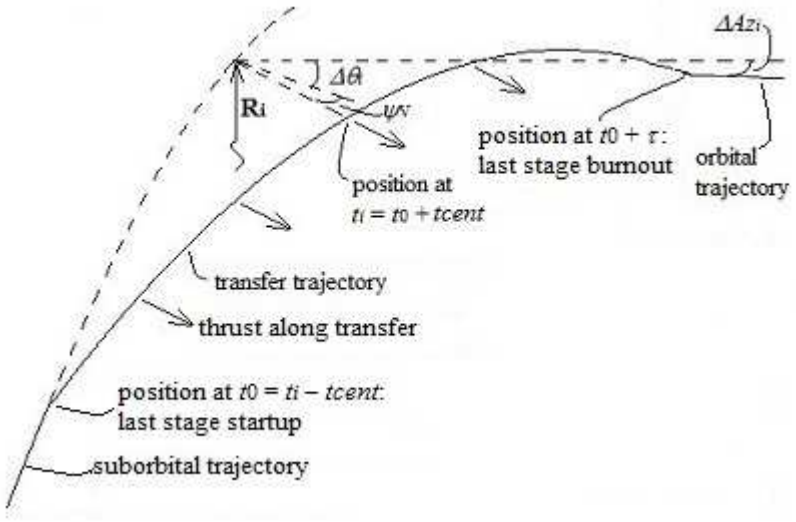


Figure 1: Synchronizing of orbit transfer by centroid time of thrust acceleration profile

Vacuum conditions may be assumed since, during transfer, atmospheric pressure is negligible. In the course of actuation of the engine, the inertial direction of propulsion, and so of the resulting acceleration, is constant. We have:

$$\Delta Vp = \int_0^\tau Ap(t)dt \tag{1}$$

As a vacuum propulsion and propellant mass table of variation in time is available, numeric integration is quite convenient. This way, the acceleration has the following calculus, along with integration: $Ap(t) = T(t)/\big(mc + mp(t)\big)$. After integration, the centroid time *tcent* of thrust acceleration profile is:

$$tcent = \frac{\int_0^\tau t.Ap(t)dt}{\int_0^\tau Ap(t)dt} = \frac{\int_0^\tau t.Ap(t)dt}{\Delta Vp} \tag{2}$$

Using this centroid time *tcent* , the start-up time is set referred to the impulse time $t_i$ [1] as $t_0 = t_i - tcent$.
However, when fixing the start-up time $t_0$, its feasibility must be verified. Before last stage start-up, the vehicle must be positioned and stabilized in the adequate inertial longitudinal angular attitude, the tipping manoeuvre. The time interval to do this is set as a constant for the mission, named *ttip*. If $Dt_at_0$ and $Dt_at_i$ are the time intervals from initial time $t_a$ of suborbital trajectory respectively till start-up time $t_0$ and impulse time $t_i$, it is required that:

$$Dt_at_0 \geq ttip \rightarrow Dt_at_i \geq ttip + tcent \tag{3}$$

Usually, Eq. (3) is satisfied at first setting of $t_0$. But, if it is not, $t_0$ and $t_i$, are re-valued, as in subsections 2.4 and 2.5.

## 2.2 Reference systems

For the characterization of the suborbital trajectory, parameters must be referred to an inertial geocentric equatorial reference frame, here called frame **G**, with axes **XG**, **YG**, **ZG**, with **ZG** pointing to the north pole. Here, this is also the inertial navigation frame.
For the quantification of the pointing angles, an inertial reference frame, called frame **V**, with axes **XV**, **YV**, **ZV**, determined by the inertial position and velocity vectors, as provided by navigation at initial time $t_a$, when already in suborbital trajectory. Axis **XV** is aligned to this position vector, and **XV** and **ZV** are in the suborbital trajectory plane, so **YV** is normal to this plane. For transformations **V** → **G**, a direction cosine matrix, called **TGV**, is used. This matrix is set by the coordinates in frame **G** of the unit vectors of the frame **V** axes, taken as column vectors:

$$\hat{\mathbf{x}}\mathbf{v}_\mathbf{G} = \mathbf{R}_{\mathbf{aG}}/\left\|\mathbf{R}_{\mathbf{aG}}\right\|;\ \ \hat{\mathbf{y}}\mathbf{v}_\mathbf{G} = \mathbf{D}/\left\|\mathbf{D}\right\|;\ \ \hat{\mathbf{z}}\mathbf{v}_\mathbf{G} = \mathbf{R}_{\mathbf{aG}} \times \mathbf{D}/\left\|\mathbf{R}_{\mathbf{aG}} \times \mathbf{D}\right\|$$
$$\mathbf{TGV} = \left(\hat{\mathbf{x}}\mathbf{v}_\mathbf{G} \quad \hat{\mathbf{y}}\mathbf{v}_\mathbf{G} \quad \hat{\mathbf{z}}\mathbf{v}_\mathbf{G}\right) \tag{4}$$

where: $\mathbf{R_{aG}}$ : Position at initial time $t_a$, in suborbital trajectory, expressed in frame **G**, $\mathbf{D} = \mathbf{V_{aG}} \times \mathbf{R_{aG}}$,

$\mathbf{V_{aG}}$ : Velocity at initial time $t_a$, in suborbital trajectory, expressed in frame **G**.

One more inertial reference frame is utilized, to set vector relations for impulsive transfer, called frame **I**, with axes **XI**, **YI**, **ZI**. Axis **XI** is aligned to geocentric radial position vector $\mathbf{R_i}$ of the vehicle at the impulse time $t_i$. Axes **XI** and **ZI** are in the suborbital trajectory plane, and **YI** has the same orientation as **YV**. Transformation from frame **I** to frame **V** is performed through a simple rotation around **YI** or **YV**, with an angle equal to the difference between true anomalies $f_i - f_a$, geocentric angular displacement of the vehicle, from time $t_a$ to time $t_i$.

## 2.3 Suborbital trajectory identification

Just after initiated the suborbital trajectory, navigation provides inertial position $\mathbf{R_{aG}}$ ($R_a = \|\mathbf{R_{aG}}\|$) and velocity $\mathbf{V_{aG}}$ ($V_a = \|\mathbf{V_{aG}}\|$) expressed in frame **G** and referred to the initial time $t_a$ of this trajectory. The vector parameters specific angular momentum $\mathbf{Hsub_G}$ ($Hsub = \|\mathbf{Hsub_G}\|$), nodal $\mathbf{Nsub_G}$ ($Nsub = \|\mathbf{Nsub_G}\|$) and eccentricity $\mathbf{esub_G}$ ($esub = \|\mathbf{esub_G}\|$), constants for the suborbital trajectory and expressed in frame **G**, are [2]:

$$\mathbf{Hsub_G} = \begin{pmatrix} Hsub_{Gx} & Hsub_{Gy} & Hsub_{Gz} \end{pmatrix}^T = \mathbf{R_{aG}} \times \mathbf{V_{aG}} \tag{5}$$

$$\mathbf{Nsub_G} = \begin{pmatrix} 0 & 0 & 1 \end{pmatrix}^T \times \mathbf{Hsub_G} = \begin{pmatrix} -Hsub_{Gy} & Hsub_{Gx} & 0 \end{pmatrix}^T$$

$$\mathbf{esub_G} = \begin{pmatrix} esub_{Gx} & esub_{Gy} & esub_{Gz} \end{pmatrix}^T = \frac{1}{\mu}\left[\left(V_a{}^2 - \frac{\mu}{R_a}\right)\mathbf{R_{aG}} - \left(\mathbf{R_{aG}} \cdot \mathbf{V_{aG}}\right)\mathbf{V_{aG}}\right] \tag{6}$$

where $\mu$ is the Earth gravitational parameter.

Also constants for the suborbital, the scalar parameters semi-major axis *asub*, semi-latus rectum *psub*, apogee ray *Raposub*, apogee speed *Vaposub*, mean motion *nsub*, inclination *Isub* and argument of perigee $\omega sub$ are [2]:

$$asub = \frac{R_a}{2 - \left(R_a . V_a{}^2 / \mu\right)} \tag{7}$$

$$psub = asub\left(1 - esub^2\right) \tag{8}$$

$$Raposub = asub(1 + esub) \tag{9}$$

$$Vaposub = \left(\frac{\mu}{psub}\right)^{1/2}\left(1 - esub\right) \tag{10}$$

$$nsub = \left(\frac{\mu}{asub^3}\right)^{1/2} \tag{11}$$

$$Isub = \arccos\left(\frac{Hsub_{Gz}}{Hsub}\right) \tag{12}$$

$$\cos(\omega sub) = \frac{\mathbf{esub_G} \cdot \mathbf{Nsub_G}}{esub.Nsub} \tag{13}$$

where: if $esub_{Gz} > 0$ then: $0 \le \omega sub < \pi$; else: $\pi \le \omega sub < 2\pi$.

The time-varying parameters trajectory angle $\beta_a$, true anomaly $f_a$ and eccentric anomaly $E_a$, for the time $t_a$ in suborbital trajectory are [2]:

$$\beta_a = \arcsin\left(\frac{\mathbf{R_{aG}} \cdot \mathbf{V_{aG}}}{R_a . V_a}\right) \tag{14}$$

$$\cos\left(f_a\right) = \frac{psub - R_a}{esub . R_a} \tag{15}$$

$$\cos(E_a) = \frac{asub - R_a}{asub.esub} \tag{16}$$

where: if $\beta_a \geq 0$ then: $0 \leq f_a \leq \pi$ and $0 \leq E_a \leq \pi$; else: $\pi < f_a < 2\pi$ and $\pi < E_a < 2\pi$.
The trajectory angle $\beta_a$ in Eq. (14) is to be positive. If not, then the vehicle is entering the suborbital trajectory already in decreasing altitude, and this is treated as fault condition. But if $\beta_a$ is positive as expected, the time interval D$t_a$*taposub*, from $t_a$ till apogee time *taposub*, is [2]:

$$Dt_a taposub = \frac{1}{nsub}\left[\pi - E_a + esub.\sin(E_a)\right] \tag{17}$$

## 2.4 Solution constraining and requirements priority

Initial propelled stages are planned so that the vehicle enters the suborbital trajectory, described in subsection 2.3, in such conditions that, through the transfer that last stage provides, the orbit requirements are fully satisfied. However, it must be considered the possibility of occurrence of dispersions in initial phases, which lead to the impossibility of requirements fulfilment. If this happens, a best possible solution is determined, taking into account a pre-established priority between inclination and eccentricity requirements. It should be kept in mind that orbit transfer is to be done by the target orbit perigee. We set the following variables:
$R_i$*bot*: Minimum impulse ray allowing orbit transfer by perigee.
*haposub*: Altitude of the suborbital trajectory apogee, corresponding to its apogee ray *Raposub* in Eq. (9).
$R_i$*top*: Maximum possible impulse ray.
$Dt_a t_i$*top*: Time interval from initial time $t_a$ till time corresponding to $R_i$*top*, in the suborbital trajectory.
$E_i$*top*: Eccentric anomaly corresponding to $R_i$*top*.
$f_i$*top*: True anomaly corresponding to $R_i$*top*.
$V_i$*top*: Vehicle speed corresponding to $R_i$*top*.
$\beta_i$*top*: Trajectory angle corresponding to $R_i$*top*.
$\Delta\theta_i$*top*: Local pitch angle, for orbit transfer without inclination change, corresponding to $R_i$*top*.
*Vsattop*: Injection speed, for orbit transfer without inclination change, corresponding to $R_i$*top*.
*Vcirtop*: Speed in a circular orbit with ray equal to $R_i$*top*.
*eorbMax*: Maximum feasible eccentricity for a target orbit.
*eorbIn*: Target orbit eccentricity value, to be used in iterative proceedings.
*VsatMin*: Minimum orbit injection speed for the target orbit, to be used in iterative proceedings.
In the course of the suborbital trajectory, in normal conditions, there should be two points of same geocentric distance $R_i$*bot*, one in the increasing altitude sector, the other in the decreasing altitude sector, where the impulsive transfer without inclination change (in relation to suborbital trajectory inclination) would lead to circular orbit with geocentric distance equal to $R_i$*bot*. So, in points above those two of minimum ray $R_i$*bot* and up to the maximum impulse ray $R_i$*top*, which in these normal conditions is the suborbital apogee ray *Raposub* in Eq. (9), the transfer without inclination change would be by the perigee of the target orbit, in which the eccentricity would increase with the increasing of the impulse ray, to say, the target orbit perigee ray. And in points under those of minimum ray $R_i$*bot*, the horizontal transfer would only be possible by the target orbit apogee, in which the eccentricity would increase with the decreasing of the impulse ray, to say, target orbit apogee ray.
Yet in normal conditions, for each point above those of minimum ray $R_i$*bot*, the introduction of orbit inclination change within the transfer, would result in target orbit in which the eccentricity decreases with the increasing, in absolute value, of the orbit inclination change; up to attain null eccentricity, after what the eccentricity would be increasing, but with transfer by apogee. If the inclination requirement is set preferential over the eccentricity requirement, the criterion here is to allow the quantification of inclination change up to the limit of circular resulting orbit. But, if the eccentricity requirement is set preferential over the inclination requirement, inclination change is quantified as to best fulfil the eccentricity requirement, with transfer by perigee. We note that the range of feasible solutions increases with the increasing of the altitude. Nevertheless, the solution that best fulfil the requirements, with priority, is associated to a unique feasible altitude. Moreover, if any of inclination value or eccentricity value

results at its respective feasibility limit, the impulsive transfer is done at the highest possible altitude which, in the above normal conditions, is the suborbital apogee altitude *haposub*; and vice-versa, if the impulsive transfer altitude results the highest possible, at least one of the two requirements is quantified at its feasibility limit.

However, due to eventual severe dispersions, conditions might be diverse from the above. Examining Eq. (3), the minimum time interval from initial time $t_a$ to impulse time $t_i$ is *ttip* + *tcent*. If in this minimum time interval the vehicle is already above that minimum ray $R_i bot$, but not beyond the suborbital apogee ($Dt_a taposub \geq ttip + tcent$), then, if the impulse ray $R_i$ is unfeasible in the increasing altitude sector, it is enough to make the transfer with $R_i$ in the decreasing altitude sector.

Now, if in the minimum time interval the vehicle is already beyond suborbital apogee ($Dt_a taposub < ttip + tcent$), yet above the minimum ray $R_i bot$ in the decreasing altitude sector, the maximum impulse ray $R_i top$ becomes smaller than the suborbital apogee ray *Raposub*. Hence, feasible solutions range becomes more constrained.

In the most adverse conditions, if the suborbital trajectory is such that it is not possible any transfer by the perigee of the target orbit, or if in the minimum time interval *ttip* + *tcent* the vehicle is already under the minimum ray $R_i bot$ in the decreasing altitude sector, then the orbit transfer is accomplished at the greatest possible ray $R_i top$, without inclination change, with horizontal orbit injection, which in this case means by the apogee of the resulting orbit.

Using results from Eqs. (1), (2), (6) to (11), (16) and (17), we have the following proceeding:

1) If $E_a < \pi$ (vehicle in the increasing altitude sector) and $Dt_a taposub \geq ttip + tcent$:

$$E_i top = \pi \tag{18}$$

$$R_i top = Raposub \tag{19}$$

$$Dt_a t_i top = Dt_a taposub \tag{20}$$

$$f_i top = \pi; \quad \Delta\theta_i top = 0; \quad Vsattop = Vaposub + \Delta Vp$$

2) Else, if $E_a \geq \pi$ or $Dt_a taposub < ttip + tcent$, the eccentric anomaly $E_i top$ is calculated first, using a time interval $\Delta t$ within a reference eccentric anomaly *Eref*; then, the remaining variables are calculated [2]:

If $E_a \geq \pi \rightarrow Eref = E_a \rightarrow \Delta t = ttip + tcent$.

Else (so, $Dt_a taposub < ttip + tcent$) $\rightarrow Eref = \pi \rightarrow \Delta t = ttip + tcent - Dt_a taposub$.

Then, with the determined *Eref* and $\Delta t$:

$$E_i top = Eref + \frac{\Delta t.nsub}{1 - esub.\cos(Eref)} \tag{21}$$

$$R_i top = asub\left(1 - esub.\cos(E_i top)\right) \tag{22}$$

$$Dt_a t_i top = ttip + tcent \tag{23}$$

$$\cos(f_i top) = \frac{psub - R_i top}{esub.R_i top} \rightarrow f_i top = 2\pi - \arccos\left(\cos(f_i top)\right);$$

$$V_i top = \left(\frac{2\mu}{R_i top} - \frac{\mu}{asub}\right)^{1/2}; \quad \beta_i top = \arctan\left(\frac{esub.\sin(f_i top)}{1 + esub.\cos(f_i top)}\right);$$

$$\Delta\theta_i top = \arcsin\left(-\frac{V_i top.\sin(\beta_i top)}{\Delta Vp}\right); \quad Vsattop = V_i top.\cos(\beta_i top) + \Delta Vp.\cos(\Delta\theta_i top)$$

3) In a circular orbit of ray $R_i top$, the speed would be: $Vcirtop = (\mu / R_i top)^{1/2}$. Now, if we have $Vsattop \leq Vcirtop$, we are in the most adverse conditions. Therefore, iterative proceedings of subsections 2.5 and 2.6 are not applied; and the time interval $Dt_a t_0$, true anomaly $f_i$, local pitch angle $\Delta\theta_i$ and local yaw angle $\psi_V$ will be as follow:

$$Dt_a t_0 = Dt_a t_i top - tcent \tag{24}$$

$$f_i = f_i top \tag{25}$$

$$\Delta\theta_i = \Delta\theta_i top \tag{26}$$

$$\psi_V = 0 \tag{27}$$

Instead, if *Vsattop* > *Vcirtop*, there is a set of solutions, with orbit transfer by its perigee. Aiming convergence to the best feasible solution, we set some feasibility limits to use within iterations. The maximum feasible eccentricity corresponds to transfer at the maximum ray, with no inclination change [2]: $eorbMax = \left(Vsattop^2 . R_i top / \mu\right) - 1$.

Then, the target orbit eccentricity *eorbIn*, to be used in iterations, may be smaller than the required *eorb*. The minimum injection speed *VsatMin* relates to transfer at maximum ray [2], with inclination change set by the priority:

$$\begin{aligned} &\text{If} \quad eorb \le eorbMax \rightarrow eorbIn = eorb \\ &\text{If} \quad eorb > eorbMax \rightarrow eorbIn = eorbMax \end{aligned} \tag{28}$$

$$\begin{aligned} &\text{If priority is inclination} \rightarrow VsatMin = \left(\frac{\mu}{R_i top}\right)^{1/2} \\ &\text{If priority is eccentricity} \rightarrow VsatMin = \left(\frac{\mu(1+eorbIn)}{R_i top}\right)^{1/2} \end{aligned} \tag{29}$$

The orbit requirements are on inclination and eccentricity. But the orbit injection speed corresponding to the required inclination depends upon the yet unknown declination at the point of impulsive transfer. Hence, it is not yet known if the limit *VsatMin* is going to impose inclination value different from the required one during iterations. Furthermore, if inclination is the priority over eccentricity, the solution to be found for the inclination may cause to eccentricity greater constraining than that caused by *eorbMax*. The iterative proceedings solve these issues.

## 2.5 Impulse ray, timing and local pitch angle

Figure 2 is a vector sketch of the impulsive transfer, with the following data referred to the impulse time $t_i$, vectors expressed in frame **I**:

$\mathbf{R_i}$: Impulse ray ($R_i = \|\mathbf{R_i}\|$).

$\mathbf{V_i}$: Vehicle velocity in the suborbital trajectory ($V_i = \|\mathbf{V_i}\|$).

$\beta_i$: Trajectory angle in the suborbital trajectory.

$\Delta\theta_i$: Local pitch angle, around vehicle's pitch axis, in plane **ZI**-**XI**, starting from **ZI**, negative if downward.

$\psi_V$: After angular displacement $\Delta\theta_i$, local yaw angle, around vehicle's yaw axis.

**ΔVp**: Velocity increment, or characteristic velocity, due to propulsion ($\Delta Vp = \|\mathbf{\Delta Vp}\|$).

$\mathbf{Vsat} = \mathbf{V_i} + \mathbf{\Delta Vp}$: Target orbit injection velocity ($Vsat = \|\mathbf{Vsat}\|$).

$\Delta Az_i$: Azimuth change in the transfer.

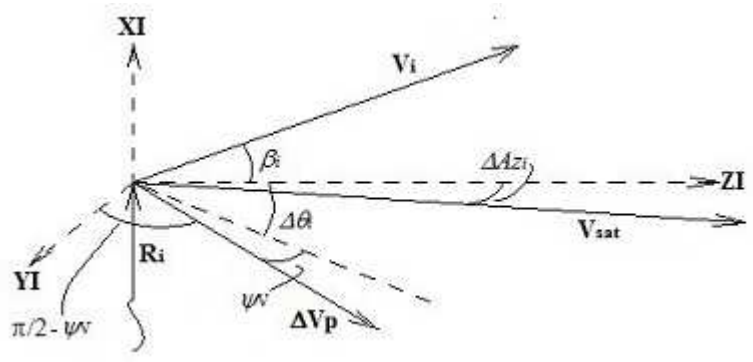


Figure 2: Vector diagram of the impulsive orbit transfer

**Primary determination of the impulse ray:**

Still using reference frame **I**, the following expressions hold for the velocities:

$$\mathbf{V_i} = V_i \left(\sin(\beta_i) \quad 0 \quad \cos(\beta_i)\right)^{\mathrm{T}} \tag{30}$$

$$\Delta\mathbf{Vp} = \Delta Vp\left(\cos(\psi_V)\sin(\Delta\theta_i) \quad \sin(\psi_V) \quad \cos(\psi_V)\cos(\Delta\theta_i)\right)^T \tag{31}$$

$$\mathbf{Vsat} = \mathbf{V_i} + \mathbf{\Delta Vp} \rightarrow Vsat^2 = V_i^2 + \Delta Vp^2 + 2\mathbf{V_i}\cdot\mathbf{\Delta Vp} \tag{32}$$

The energy and angular momentum equations, holding for the suborbital trajectory, are applied for the time $t_i$ [3]:

$$V_i^2 - \frac{2\mu}{R_i} = -\frac{\mu}{asub} \tag{33}$$

$$V_i R_i \cos(\beta_i) = Hsub \tag{34}$$

If the orbit injection velocity **Vsat** is to be in the local horizontal plane, then:

$$V_i \sin(\beta_i) + \Delta Vp.\cos(\psi_V)\sin(\Delta\theta_i) = 0 \tag{35}$$

$$\left(V_i \cos(\beta_i) + \Delta Vp.\cos(\psi_V)\cos(\Delta\theta_i)\right)^2 + \left(\Delta Vp.\sin(\psi_V)\right)^2 = Vsat^2 \tag{36}$$

If the target orbit eccentricity should be *eorbIn*, given by Eq. (28), with $R_i$ becoming its perigee distance, then [2]:

$$Vsat^2 = \frac{\mu(1+eorbIn)}{R_i} \tag{37}$$

The manipulation of Eqs. (30) to (37), aiming the determination of $R_i$, lead to the following 3rd order equation [3]:

$$R_i^3 + A_1 R_i^2 + A_2 R_i + A_3 = 0 \tag{38}$$

where: $A_1 = -\frac{2(3+eorbIn)}{F}$; $F = \frac{1}{asub} + \frac{\Delta Vp^2}{\mu}$;

$$A_2 = \frac{(3+eorbIn)^2 + 4\left(\frac{\Delta Vp.\sin(\psi_V)Hsub}{\mu}\right)^2}{F^2}; \quad A_3 = -\frac{4Hsub^2(1+eorbIn)}{\mu F^2}.$$

$\Delta Vp$ is a flight parameter, pre-determined as in Eq. (1), *asub* and *Hsub* are given by Eqs. (7) and (5). The local yaw angle $\psi_V$ is determined in the following subsection 2.6, but using the value of $R_i$ now being determined. Hence, in the first iteration, a null or nominal value for $\psi_V$ is used here. Afterwards, $\psi_V$ and $R_i$ are alternately and iteratively calculated, the output of each iteration being the input to the next, till some condition is fulfilled; for instance, the difference between the outputs of consecutive iterations are under certain negligible maxima. But, as the proceedings are set here, a determination of $R_i$ should be the first and the last one.

Mathematically, Eq. (38) may have up to three real solutions, but only one should have feasible physical meaning. We take the auxiliary variables $P = \left(A_1^2 - 3A_2\right)/9$, $Q = \left(9A_1A_2 - 2A_1^3 - 27A_3\right)/54$, and the three situations bellow [4]:

1st) $Q^2 - P^3 \cong 0$: All the three roots are real, the second one duplicate: $R_i = 2Q^{1/3} - A_1/3$, $R_i = -Q^{1/3} - A_1/3$.

2nd) 1st situation does not hold and $Q^2$–$P^3$>0: One root is real: $R_i = \left(Q + (Q^2 - P^3)^{1/2}\right)^{1/3} + \left(Q - (Q^2 - P^3)^{1/2}\right)^{1/3} - A_1/3$

3rd) 1st situation does not hold and $Q^2$–$P^3$<0: All three roots are real:

$$R_i = 2P^{1/2}\cos\left(\frac{S}{3}\right) - \frac{A_1}{3}, \quad R_i = 2P^{1/2}\cos\left(\frac{S}{3} + \frac{2\pi}{3}\right) - \frac{A_1}{3}, \quad R_i = 2P^{1/2}\cos\left(\frac{S}{3} + \frac{4\pi}{3}\right) - \frac{A_1}{3} \tag{39}$$

where: $S = \arccos\left(Q/P^{3/2}\right)$.

In the above 1st and the 3rd situations, the solution should be selected by testing the physical meaning, for instance, which one is the closest to a pre-established reasonable value. Nevertheless, in all cases we have simulated, the 3rd situation holds and its last root listed in Eq. (39) is the solution.

**Timing, fault conditions and impulse ray adjustment:**
Using $E_i top$ (or Eq. (18) or Eq. (21)), $R_i top$ (or Eq. (19) or Eq. (22)), $Dt_a t_i top$ (or Eq. (20) or Eq. (23)), $E_a$ (Eq. (16)), *asub* (Eq. (7)), *esub* (Eq. (6)), *nsub* (Eq. (11)), *tcent* (Eq. (2)) and tipping time *ttip*, we set possible adjustment in impulse ray $R_i$, its corresponding eccentric anomaly $E_i$ and time interval $Dt_a t_i$, from initial time $t_a$ to impulse time $t_i$:
1st situation) $R_i \geq R_i top$ (fault: insufficient energy; this may occur even with the previous proceedings in subsection 2.4): Transfer at the maximum impulse ray: $E_i = E_i top$, $R_i = R_i top$, $Dt_a t_i = Dt_a t_i top$.
2nd situation) $R_i < R_i top$: $E_i$ is calculated, at first for increasing altitude [2]: $E_i = \arccos\left((asub - R_i)/(asub.esub)\right)$.

But, if results $E_i < E_a$ or if $E_i top > \pi$ (fault: insufficient time in the increasing altitude sector), then $E_i$ is recalculated for the decreasing altitude sector [3]: $E_i = 2\pi - E_i$. With the $E_i$ determined, $Dt_a t_i$ is calculated [2]:

$$Dt_a t_i = \frac{1}{nsub}\left\{E_i - E_a - esub\left[\sin(E_i) - \sin(E_a)\right]\right\} \tag{40}$$

But, if results $Dt_a t_i < ttip, + tcent$ (fault: insufficient time; because of proceedings in subsection 2.4, this can only occur if still in increasing altitude sector), then $E_i$ is recalculated for the decreasing altitude sector: $E_i = 2\pi - E_i$. Then, $Dt_a t_i$ is recalculated as in Eq. (40).
For both situations above, the time interval $Dt_a t_0$, from initial time $t_a$ to start-up time $t_0$, is finally calculated:

$$Dt_a t_0 = Dt_a t_i - tcent \tag{41}$$

**Local pitch angle, orbit injection speed and effective eccentricity:**
Using $R_i$, $E_i$, *psub* (Eq. (8)), *esub* (Eq. (6)) and *asub* (Eq. (7)), we determine the true anomaly $f_i$, the vehicle speed $V_i$ and the trajectory angle $\beta_i$, at impulse time $t_i$ [2] :

$$\cos(f_i) = \frac{psub - R_i}{esub.R_i} \tag{42}$$

$$V_i = \left(\frac{2\mu}{R_i} - \frac{\mu}{asub}\right)^{1/2} \quad ; \quad \beta_i = \arctan\left(\frac{esub.\sin(f_i)}{1 + esub.\cos(f_i)}\right)$$

where: if $E_i < \pi$, then $0 \leq f_i < \pi$; else $\pi \leq f_i < 2\pi$.
If impulse ray $R_i$ has been modified, then the target orbit eccentricity is different from that used for $R_i$ primary determination. Anyway, orbit injection is to be horizontal; hence, respectively from Eq. (35) and Eq. (36), we have the local pitch angle and the target orbit injection speed:

$$\Delta\theta_i = \arcsin\left(-\frac{V_i \sin(\beta_i)}{\Delta Vp.\cos(\psi_V)}\right) \tag{43}$$

$$Vsat = \left(\left(V_i \cos(\beta_i) + \Delta Vp.\cos(\psi_V)\cos(\Delta\theta_i)\right)^2 + \left(\Delta Vp.\sin(\psi_V)\right)^2\right)^{1/2} \tag{44}$$

The resulting effective eccentricity, which is not needed in the proceedings, can be obtained just for information [2]:

$$eorbEf = \frac{Vsat^2 R_i}{\mu} - 1$$

## 2.6 Azimuth change and local yaw angle

In subsection 2.5, with a previous value of the local yaw angle $\psi_V$, we have calculated the impulse ray $R_i$, the vehicle speed $V_i$, the trajectory angle $\beta_i$, the true anomaly $f_i$, the orbit injection speed *Vsat* and the local pitch angle $\Delta\theta_i$. In this subsection, other values for the orbit injection speed and the local pitch angle are calculated, named respectively *VsatI* and $\Delta\theta_i I$, using and keeping unchanged the remaining variables above; and a new value for $\psi_V$ is generated.
In the orbit transfer, there should be an inclination change from the suborbital inclination *Isub* to the target orbit required inclination *Iorb*. This inclination change corresponds to an azimuth change $\Delta Az_i$, from the suborbital azimuth $Aze_i$ at impulse time $t_i$ to the target orbit azimuth $Azf_i$ at the same time, or $\Delta Az_i = Azf_i - Aze_i$; which depends upon transfer geographical localization. As shows Fig. 2 and regarding that here the orbit injection speed is named *VsatI* instead of *Vsat*, to achieve this azimuth change, the vehicle should be pointed with local yaw angle $\psi_V$, so that:

$$VsatI.\sin(\Delta Az_i) = \Delta Vp.\sin(\psi_V) \tag{45}$$

**Primary determination of the azimuth change:**

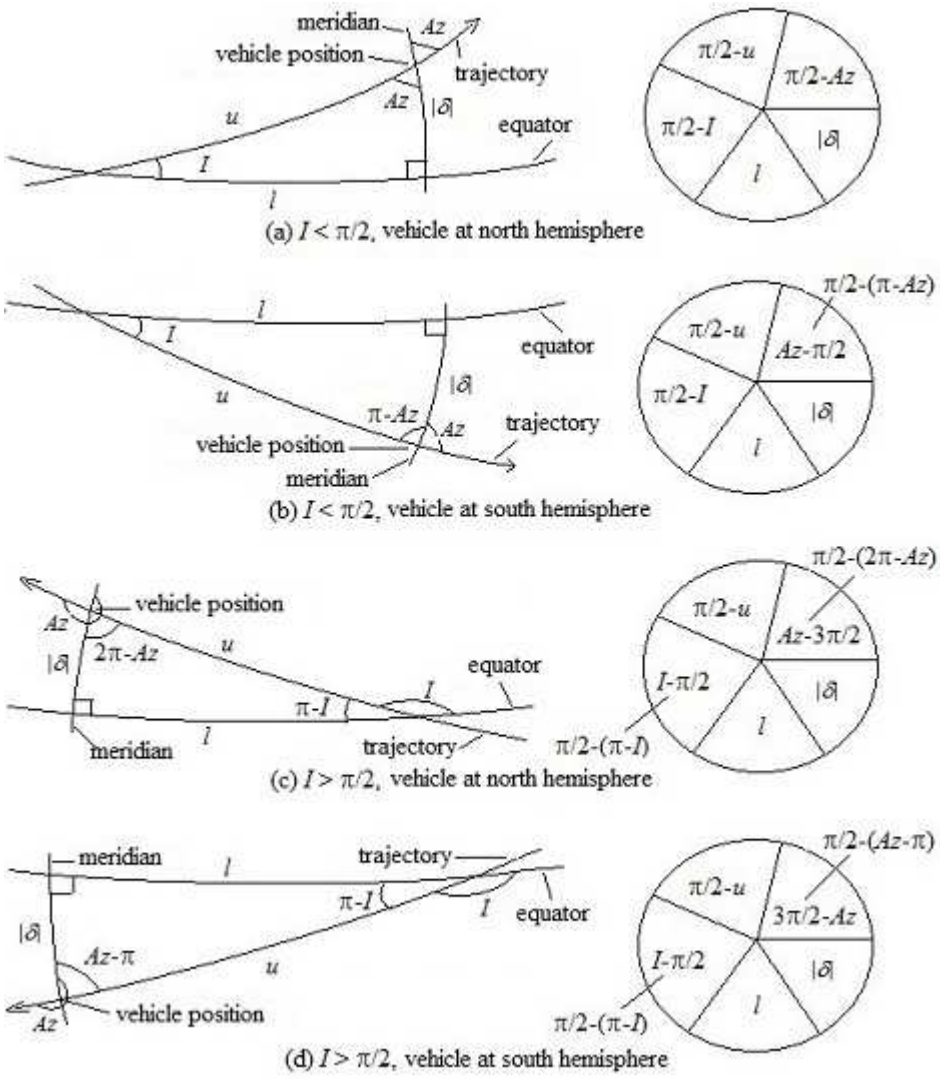


Figure 3: Trajectory spherical trigonometry

Figure 3 illustrates, for a generic vehicle position in a trajectory, the right spherical triangle delimited by the equatorial plane, the local meridian plane and the trajectory plane. Four situations are illustrated, varying the trajectory plane inclination, which is in the range from 0 to π radians, and the geographical position of the vehicle:

(a): Inclination less than π/2 (progressive), and position at the north hemisphere.
(b): Inclination less than π/2 (progressive), and position at the south hemisphere.
(c): Inclination greater than π/2 (regressive), and position at the north hemisphere.
(d): Inclination greater than π/2 (regressive), and position at the south hemisphere.

In all the above situations, it should be noticed that the shown variables and expressions hold as well if the considered position is in increasing latitude ($\pi/2 \leq u < \pi$, at the south hemisphere; $0 \leq u < \pi/2$, at the north hemisphere) or in decreasing latitude ($\pi/2 \leq u < \pi$, at the north hemisphere; $0 \leq u < \pi/2$, at the south hemisphere) sector of the trajectory. The concerning angular variables are:

$|\delta|$ (in the meridian plane): Absolute value of the declination at the current position.
$l$ (in the equatorial plane): Equatorial angular displacement, from last equator crossing up to the current meridian.
$I$ (between equatorial and trajectory planes): Trajectory plane inclination.
$u$ (in the trajectory plane): Trajectory angular displacement, from last equator crossing up to the current position.
$Az$ (between meridian and trajectory planes): Trajectory current azimuth.

The circles for each situation in Fig. 3, suitably shared in the shown angles, are to guide the application of Napier rules [5] for right spherical triangles. So, we state:

Situation (a): $\sin(\pi/2 - I) = \cos(|\delta|)\cos(\pi/2 - Az)$.
Situation (b): $\sin(\pi/2 - I) = \cos(|\delta|)\cos(Az - \pi/2)$.
Situation (c): $\sin(I - \pi/2) = \cos(|\delta|)\cos(Az - 3\pi/2)$.
Situation (d): $\sin(I - \pi/2) = \cos(|\delta|)\cos(3\pi/2 - Az)$.

From any of these four statements, results: $\sin(Az) = \cos(I)/\cos(|\delta|)$.

From the above value of its sine, the value of the azimuth is determined considering its corresponding quadrant, which is determined by the inclination type (or $I < \pi/2$, or $I > \pi/2$), and by the trajectory sector of current position (or in increasing latitude sector, or in decreasing latitude sector). Table 1 presents the azimuth determination in relation to inclination type and latitude variation related sector.

Table 1: Azimuth determination

| Inclination type | Latitude variation | Azimuth quadrant | Azimuth: $Az$ |
|---|---|---|---|
| $I < \pi/2$ | increasing | 1st | $\arcsin\left(\frac{\cos(I)}{\cos(\lvert\delta\rvert)}\right)$ |
| | decreasing | 2nd | $\pi - \arcsin\left(\frac{\cos(I)}{\cos(\lvert\delta\rvert)}\right)$ |
| $I > \pi/2$ | decreasing | 3rd | |
| | increasing | 4th | $2\pi + \arcsin\left(\frac{\cos(I)}{\cos(\lvert\delta\rvert)}\right)$ |

We assume that the transfer is in such a way that, at the impulsive transfer position, if the latitude is or increasing or decreasing in the origin trajectory, then it also will be respectively or increasing or decreasing in the target trajectory. This corresponds to the option for the manoeuvre with less azimuth change, in eventual cases where it could be possible to choose between two opposed manoeuvres which would lead to trajectories with the same inclination.

However, there is a constraint for the target orbit inclination *Iorb*, which should be such that the trajectory can attain the impulsive transfer latitude $\delta_i$, constraint which may also be deduced from the azimuth column in Table 1:

$|\cos(Iorb)| \leq \cos(|\delta_i|) \rightarrow |\delta_i| \leq Iorb \leq \pi - |\delta_i|$.

Then, at each iteration we determine a value *IorbIn* for the target orbit inclination, to use in place of *Iorb*, as follows:

$$\begin{aligned} &\text{If } |\delta_i| \leq Iorb \leq \pi - |\delta_i| \rightarrow IorbIn = Iorb \\ &\text{If } Iorb < |\delta_i| \rightarrow IorbIn = |\delta_i| \\ &\text{If } Iorb > \pi - |\delta_i| \rightarrow IorbIn = \pi - |\delta_i| \end{aligned} \tag{46}$$

After the above precaution, Table 2 presents the possible transfer cases, with corresponding azimuth changes.

Table 2: Orbit transfer cases and azimuth changes

| Latitude | Inclination | | Azimuth change: $\Delta Az_i = Azf_i - Aze_i$ |
|---|---|---|---|
| | Origin | Target | |
| Increasing | $Isub < \pi/2$ | $IorbIn < \pi/2$ | $\arcsin\left(\frac{\cos(IorbIn)}{\cos(\lvert\delta_i\rvert)}\right) - \arcsin\left(\frac{\cos(Isub)}{\cos(\lvert\delta_i\rvert)}\right)$ |
| | $Isub > \pi/2$ | $IorbIn > \pi/2$ | |
| | $Isub < \pi/2$ | $IorbIn > \pi/2$ | $2\pi + \arcsin\left(\frac{\cos(IorbIn)}{\cos(\lvert\delta_i\rvert)}\right) - \arcsin\left(\frac{\cos(Isub)}{\cos(\lvert\delta_i\rvert)}\right)$ |
| | $Isub > \pi/2$ | $IorbIn < \pi/2$ | $\arcsin\left(\frac{\cos(IorbIn)}{\cos(\lvert\delta_i\rvert)}\right) - 2\pi - \arcsin\left(\frac{\cos(Isub)}{\cos(\lvert\delta_i\rvert)}\right)$ |
| Decreasing | any | any | $-\arcsin\left(\frac{\cos(IorbIn)}{\cos(\lvert\delta_i\rvert)}\right) + \arcsin\left(\frac{\cos(Isub)}{\cos(\lvert\delta_i\rvert)}\right)$ |

Examining Table 2, we conclude that the cosine and the sine of the azimuth change are, respectively:

$$\cos(\Delta Az_i) = \cos\left(\arcsin\left(\frac{\cos(IorbIn)}{\cos(\lvert\delta_i\rvert)}\right) - \arcsin\left(\frac{\cos(Isub)}{\cos(\lvert\delta_i\rvert)}\right)\right) \tag{47}$$

$$\sin(\Delta Az_i) = \pm\sin\left(\arcsin\left(\frac{\cos(IorbIn)}{\cos(\lvert\delta_i\rvert)}\right) - \arcsin\left(\frac{\cos(Isub)}{\cos(\lvert\delta_i\rvert)}\right)\right) \tag{48}$$

where the positive sign is applicable if the transfer is in increasing latitude, and the negative sign if in decreasing latitude. To find out if it is increasing or decreasing, we let the variable $U_i$ be the vehicle angular displacement from the last virtual transition by the least latitude position ($\pi/2$ radian before the ascending node) up to impulsive transfer position, in the suborbital trajectory; and check the value of $U_i$. This translates to:

$$\begin{aligned} &U_i = (\pi/2 + \omega sub + f_i)\,\text{modulo}(2\pi) \\ &\text{If} \quad U_i \le \pi \rightarrow \quad \text{transfer in increasing latitude} \\ &\text{Else} \rightarrow \quad \text{transfer in decreasing latitude} \end{aligned} \tag{49}$$

However, we do not know yet the value of $|\delta_i|$. Getting back to Fig. 3 and applying once more a Napier rule [5]:

1) For $I < \pi/2$ → $\sin(|\delta|) = \cos(\pi/2 - I)\cos(\pi/2 - u)$.
2) For $I > \pi/2$ → $\sin(|\delta|) = \cos(I - \pi/2)\cos(\pi/2 - u)$.

As $|\delta|$ can only be in the 1st quadrant, from any of both above expressions yields: $|\delta| = \arcsin(\sin(I)\sin(u))$.

So, letting the variable $u_i$ be the vehicle angular displacement from the last virtual cross by equator plane up to impulsive transfer position, in the suborbital trajectory, we have:

$$u_i = (\omega sub + f_i)\,\text{modulo}(\pi); \quad |\delta_i| = \arcsin(\sin(Isub)\sin(u_i)) \tag{50}$$

Resuming, the azimuth change $\Delta Az_i$ is obtained by means of Eqs. (46) to (50), where *Isub*, $\omega sub$ and $f_i$ are given respectively by Eqs. (12), (13) and (42), and Iorb is a given parameter.

**Orbit injection velocity and azimuth adjustment:**

With the orbit injection velocity now named **VsatI** instead of **Vsat**, and the local pitch angle now named $\Delta\theta_i I$ instead of $\Delta\theta_i$, we obtain from Eqs. (30), (31) and (32):

$$VsatI^2 = V_i^2 + \Delta Vp^2 + 2V_i\Delta Vp\left[\sin(\beta_i)\cos(\psi_V)\sin(\Delta\theta_i I) + \cos(\beta_i)\cos(\psi_V)\cos(\Delta\theta_i I)\right] \tag{51}$$

Expressing the null vertical component of **VsatI**, as in Eq. (35), and its component in **ZI**, we get, respectively:

$$V_i \sin(\beta_i) + \Delta Vp.\cos(\psi_V)\sin(\Delta\theta_i I) = 0 \rightarrow \cos(\psi_V)\sin(\Delta\theta_i I) = -\frac{V_i \sin(\beta_i)}{\Delta Vp} \quad (52)$$

$$VsatI.\cos(\Delta Az_i) = V_i \cos(\beta_i) + \Delta Vp.\cos(\psi_V)\cos(\Delta\theta_i I) \rightarrow \cos(\psi_V)\cos(\Delta\theta_i I) = \frac{VsatI.\cos(\Delta Az_i) - V_i \cos(\beta_i)}{\Delta Vp} \quad (53)$$

Applying Eqs. (52) and (53) in Eq. (51), and developing, we come to the 2nd order equation in *VsatI*:

$$VsatI^2 - 2V_i \cos(\Delta Az_i)\cos(\beta_i)VsatI + V_i^2 - \Delta Vp^2 = 0 \quad (54)$$

The solutions for Eq. (54) and the condition for real solution are, respectively:

$$VsatI = V_i \cos(\Delta Az_i)\cos(\beta_i) \pm \left[V_i^2 (\cos(\Delta Az_i))^2 (\cos(\beta_i))^2 - V_i^2 + \Delta Vp^2\right]^{1/2} \quad (55)$$

$$(\cos(\Delta Az_i))^2 \geq \left(V_i^2 - \Delta Vp^2\right) / \left(V_i \cos(\beta_i)\right)^2 \quad (56)$$

If the cosine of $\Delta Az_i$, given by Eq. (47), does not fulfil Eq. (56), which also means that the 2nd side of Eq. (56) can only be positive, then we assume $|\Delta Az_i| \leq \pi/2$, and proceed the following adjustments in the values of cosine and sine of $\Delta Az_i$, where the sign of the sine is preserved as of its previous value:

$$\cos(\Delta Az_i) = \left(V_i^2 - \Delta Vp^2\right)^{1/2} / \left(V_i \cos(\beta_i)\right)$$

$$\text{If} \quad \sin(\Delta Az_i) \geq 0 \rightarrow \sin(\Delta Az_i) = \sin\left(\arccos\left(\cos(\Delta Az_i)\right)\right)$$

$$\text{Else} \quad \rightarrow \sin(\Delta Az_i) = \sin\left(-\arccos\left(\cos(\Delta Az_i)\right)\right)$$

After the above eventual adjustments, if Eq. (55) gives two distinct solutions, the criterion here is to select that which is closest to the value of *Vsat* given by Eq. (44). Now, if the selected value of *VsatI* is less than *VsatMin* given by Eq. (29), then we adjust *VsatI* and, accordingly and using Eq. (54), adjust $\Delta Az_i$, yet preserving the current sign of its sine:

$$VsatI = VsatMin$$

$$\cos(\Delta Az_i) = \left(VsatI^2 + V_i^2 - \Delta Vp^2\right) / \left(2V_i \cos(\beta_i)VsatI\right)$$

$$\text{If} \quad \sin(\Delta Az_i) \geq 0 \rightarrow \sin(\Delta Az_i) = \sin\left(\arccos\left(\cos(\Delta Az_i)\right)\right)$$

$$\text{Else} \quad \rightarrow \sin(\Delta Az_i) = \sin\left(-\arccos\left(\cos(\Delta Az_i)\right)\right)$$

**Local yaw angle and effective inclination:**
From Eqs. (52) and (53), we obtain:

$$\Delta\theta_i I = \arctan\left(-\frac{\left(V_i \sin(\beta_i)\right)}{\left(VsatI.\cos(\Delta Az_i) - V_i \cos(\beta_i)\right)}\right)$$

Then, replacing $\Delta\theta_i$ with $\Delta\theta_i I$ in Eqs (45) and (52), the local yaw angle $\psi_V$ is identified:

$$\sin(\psi_V) = VsatI.\sin(\Delta Az_i) / \Delta Vp \quad (57)$$

$$\cos(\psi_V) = -\left(V_i \sin(\beta_i)\right) / \left(\Delta Vp.\sin(\Delta\theta_i I)\right) \quad (58)$$

The resulting effective inclination *IorbEf*, which is not needed in the proceedings, can be obtained just for information, replacing *IorbIn* with *IorbEf* in Eqs. (47), (48) and (49) which, after manipulation, yields:

$$IorbEf = \arccos\left(\sin\left(\arcsin\left(\frac{\cos(Isub)}{\cos(|\delta_i|)}\right) \pm \Delta Az_i\right)\cos(|\delta_i|)\right)$$

where the positive sign is applicable if $U_i \leq \pi$; and the negative sign if $U_i > \pi$.

### 2.7 Angular attitude in navigation reference system

In frame **I**, the attitude at transfer time is expressed by angles $\Delta\theta_i$ (or Eq. (26) or Eq. (43)) and $\psi_V$ (or Eq. (27) or Eqs. (57) and (58)). Using the true anomalies $f_i$ (or Eq. (25) or Eq. (42)) and $f_a$ (Eq. (15)), we get the attitude expressed in frame **V**, with pitch angle $\theta_V$ and yaw angle the same $\psi_V$. As we consider as null attitude when the vehicle body frame is coincident with the inertial reference frame but, by convenience, we measured $\Delta\theta_i$ starting from **ZI** instead of **XI**, now we introduce an off-set of $-\pi/2$ in the rotation around **YI** or **YV**. So: $\theta_V = \Delta\theta_i - (f_i - f_a) - \pi/2$ .

The vehicle longitudinal orientation in frame **V** is: $\mathbf{L_V} = (\cos(\psi_V)\cos(\theta_V) \quad \sin(\psi_V) \quad -\cos(\psi_V)\sin(\theta_V))^T$ .

Using the matrix **TGV** in Eq. (4), the longitudinal orientation is transformed to navigation frame **G**:

$$\mathbf{L_G} = (L_{Gx} \quad L_{Gy} \quad L_{Gz})^T = (\cos(\psi_G)\cos(\theta_G) \quad \sin(\psi_G) \quad -\cos(\psi_G)\sin(\theta_G))^T = \mathbf{TGV}.\mathbf{L_V}$$

where $\theta_G$ and $\psi_G$ are, respectively, the pitch and yaw attitude angles, referred to frame **G**, to be used at transfer time. The determination of their values, from the $\mathbf{L_G}$ components, is mission dependent and should be done carefully in identifying their correct quadrants. Vehicle should be pointed and stabilized at this attitude within time interval $Dt_at_0$, set forth or by Eq. (24) or by Eq. (41).

## 3. Simulations

A software prototype was built for testing purposes on the developed pointing method. This prototype runs within an already existing simulator for launcher flight, providing fair assessment conditions. Several test cases have been performed, using two launch missions, one with suborbital trajectory in decreasing latitude, the other in increasing latitude. Table 3 lists some characteristics of the suborbital trajectory and the last stage for each mission.

Table 3: Suborbital trajectory and last stage characteristics

| | Mission → | M1 | M2 |
|---|---|---|---|
| Suborbital trajectory | Time-varying latitude | decreasing | increasing |
| | Inclination: *Isub* (deg) | 13.6556 | 14.6205 |
| | Specific angular momentum: *Hsub* ($km^2/s$) | 30104.16 | 28361.37 |
| | Initial ray: *Ra* (km) | 6620.254 | 6660.724 |
| | Apogee ray: *Raposub* (km) | 7197.389 | 7065.621 |
| | Apogee altitude: *haposub* (km) | 819.250 | 687.482 |
| | Apogee declination: *δaposub* (deg) | −6.1942 | +1.4733 |
| | Time to apogee: $Dt_ataposub$ (s) | 463.430 | 373.896 |
| | Tipping time: *ttip* (s) | 60 | 60 |
| Last stage | Centroid time of thrust acceleration profile: *tcent* (s) | 42.468 | 42.687 |
| | Characteristic speed: *ΔVp* (km/s) | 3.376259 | 3.613275 |

In all cases shown here, it has been set to stop iterations when, within two consecutive iterations, the difference between the respective impulse rays $R_i$ is less than $10^{-4}$ km, and between the respective local yaw angles $\psi_G$ is less

than $10^{-4}$ radian. In the tables below, values presented as accomplished inclination and accomplished eccentricity are the determined by the launcher flight simulator, in proceedings after finishing of the pointing method actuation.
Tables 4 and 5 show, respectively for variations on M1 and M2, cases in which the inclination and eccentricity requirements could be fully performed. For both M1 and M2, initial ascending phases are configured to attain suborbital trajectory with inclination near to the respective required target orbit inclination, and in such conditions that, with the last stage, a circular orbit in pre-established altitude is achieved. Thus, Tables 4 and 5 have the eccentricity values nearby zero. Except for cases M1a and M2a, each eccentricity value is set near the feasibility limit for the corresponding inclination value. Besides, cases M1b, M1f, M2b and M2f have inclination values set near the corresponding feasibility limits for null eccentricity. Compliance between effective values, given by the pointing prototype, and corresponding accomplished values, given by the launcher flight simulator, can be verified.

Table 4: Cases on variations of M1, without constraining actuation

| Case → | M1a | M1b | M1c | M1d | M1e | M1f |
|---|---|---|---|---|---|---|
| Required/effective inclination: *IorbEf* (deg) | 14 | 7 | 10 | 14 | 18 | 22 |
| Accomplished inclination (deg) | 14.00 | 7.00 | 10.01 | 14.01 | 18.00 | 22.00 |
| Required/effective eccentricity: *eorbEf* | 0 | 0 | 0.02 | 0.03 | 0.02 | 0 |
| Accomplished eccentricity | 0.00053 | 0.00065 | 0.01993 | 0.02995 | 0.01996 | 0.00068 |
| Impulsive transfer altitude: $h_i$ (km) | 743.104 | 808.673 | 807.530 | 815.235 | 811.564 | 816.788 |
| Impulsive transfer declination: $\delta_i$ (deg) | −4.9637 | −5.7441 | −5.7201 | −5.9179 | −5.8110 | −5.9781 |
| Azimuth change: $\Delta Az_i$ (deg) | +0.3694 | −8.4022 | −4.2044 | +0.3817 | +4.6868 | +8.9111 |
| Iterations | 3 | 13 | 6 | 3 | 6 | 9 |

Table 5: Cases on variations of M2, without constraining actuation

| Case → | M2a | M2b | M2c | M2d | M2e | M2f |
|---|---|---|---|---|---|---|
| Required/effective inclination: *IorbEf* (deg) | 14 | 6 | 10 | 14 | 18 | 24 |
| Accomplished inclination (deg) | 14.00 | 6.00 | 10.00 | 14.00 | 18.00 | 24.00 |
| Required/effective eccentricity: *eorbEf* | 0 | 0 | 0.02 | 0.03 | 0.02 | 0 |
| Accomplished eccentricity | 0.00044 | 0.00055 | 0.01988 | 0.02987 | 0.01987 | 0.00061 |
| Impulsive transfer altitude: $h_i$ (km) | 614.174 | 675.186 | 678.620 | 684.898 | 670.314 | 685.971 |
| Impulsive transfer declination: $\delta_i$ (deg) | +0.1511 | +0.9351 | +1.0166 | +1.2269 | +0.8370 | +1.2849 |
| Azimuth change: $\Delta Az_i$ (deg) | +0.6205 | +8.6643 | +4.6372 | +0.6228 | −3.3842 | −9.4025 |
| Iterations | 3 | 7 | 5 | 3 | 5 | 7 |

Tables 6 and 7 show, respectively for variations on M1 and M2, cases in which the inclination and eccentricity requirements could not be fully performed. Therefore, for each inclination/eccentricity requirements pair, two tests results are shown, with priority set respectively to one and other requirement. Now, effective values may differ from the corresponding required values, according to the feasibility conditions and the chosen priority. In cases M1aI, M1aE, M2aI and M2aE, the required inclination is unfeasible, regardless the priority and the required eccentricity, whereas the required eccentricity may be feasible, depending on priority setting and required inclination. In cases M1bI, M1bE, M2bI and M2bE, the required inclination may be feasible, depending on priority setting and required eccentricity, whereas the required eccentricity is unfeasible, regardless the priority and the required inclination. In cases M1cI, M1cE, M2cI and M2cE, both requirements are unfeasible, regardless the priority setting and the respective other requirement value. Examining effective and accomplished values, we verify that a requirement set with priority is fully performed if it is feasible, and performed up to a feasibility limit if it is not feasible. We also verify that a requirement not set with priority is at least partially performed, provided that the value of the other requirement does not achieve its feasibility limit. When this feasibility limit is achieved by the requirement set with priority, the value of the other requirement corresponds to or null eccentricity (cases M1aI, M1cI, M2aI and M2cI), or null inclination change (cases M1bE, M1cE, M2bE and M2cE), according to which is the requirement. As verified above in Tables 4 and 5, we also verify in Tables 6 and 7 the compliance between effective and accomplished values. As set forth in Subsection 2.4, when any requirement achieves its feasibility limit, the orbit transfer is performed at

the highest possible altitude, which in cases shown here is the respective suborbital apogee altitude *haposub*, once the minimum time to impulsive transfer *ttip+tcent* is less than the time to suborbital apogee $Dt_a$*taposub* in all cases.

Table 6: Cases on variations of M1, with constraining actuation

| Case → | M1aI | M1aE | M1bI | M1bE | M1cI | M1cE |
|---|---|---|---|---|---|---|
| Required inclination: *Iorb* (deg) | 0 | 0 | 10 | 10 | 180 | 180 |
| Required eccentricity: *eorb* | 0.01 | 0.01 | 0.90 | 0.90 | 0.90 | 0.90 |
| Priority (Inclination/Eccentricity) | Inc | Ecc | Inc | Ecc | Inc | Ecc |
| Effective inclination: *IorbEf* (deg) | 6.9390 | 7.7741 | 10 | *Isub* | 22.0980 | *Isub* |
| Accomplished inclination (deg) | 6.94 | 7.78 | 10.01 | 13.66 | 22.10 | 13.66 |
| Effective eccentricity: *eorbEf* | 0 | 0.01 | 0.02443 | 0.03171 | 0 | 0.03171 |
| Accomplished eccentricity | 0.00073 | 0.00995 | 0.02437 | 0.03166 | 0.00072 | 0.03166 |
| Impulsive transfer altitude | *haposub* | *haposub* | *haposub* | *haposub* | *haposub* | *haposub* |
| Impulsive transfer declination | *δaposub* | *δaposub* | *δaposub* | *δaposub* | *δaposub* | *δaposub* |
| Azimuth change: $\Delta Az_i$ (deg) | −9.0601 | −7.4869 | −4.32786 | 0 | +9.0601 | 0 |
| Iterations | 3 | 3 | 3 | 2 | 3 | 2 |

Table 7: Cases on variations of M2, with constraining actuation

| Case → | M2aI | M2aE | M2bI | M2bE | M2cI | M2cE |
|---|---|---|---|---|---|---|
| Required inclination: *Iorb* (deg) | 0 | 0 | 10 | 10 | 180 | 180 |
| Required eccentricity: *eorb* | 0.01 | 0.01 | 0.90 | 0.90 | 0.90 | 0.90 |
| Priority (Inclination/Eccentricity) | Inc | Ecc | Inc | Ecc | Inc | Ecc |
| Effective inclination: *IorbEf* (deg) | 5.2563 | 6.8845 | 10 | *Isub* | 24.0916 | *Isub* |
| Accomplished inclination (deg) | 5.26 | 6.89 | 10.00 | 14.62 | 24.09 | 14.62 |
| Effective eccentricity: *eorbEf* | 0 | 0.01 | 0.02367 | 0.03122 | 0 | 0.03122 |
| Accomplished eccentricity | 0.00063 | 0.00989 | 0.02355 | 0.03109 | 0.00064 | 0.03109 |
| Impulsive transfer altitude | *haposub* | *haposub* | *haposub* | *haposub* | *haposub* | *haposub* |
| Impulsive transfer declination | *δaposub* | *δaposub* | *δaposub* | *δaposub* | *δaposub* | *δaposub* |
| Azimuth change: $\Delta Az_i$ (deg) | 9.5015 | 7.8219 | 4.6557 | 0 | −9.5015 | 0 |
| Iterations | 3 | 3 | 3 | 2 | 3 | 2 |

## 4. Conclusion

Simulations show compliance with specifications set forth in the pointing method development. The results in all tests, some of which are depicted in Section 3, present suitable precision. Regarding that the developed algorithm is a critical application to run in flight, we stand out its following characteristics:

1) Treating for any conditions in flight, including the adverse ones resulting from severe dispersions, with generation of solutions addressing safety and best possible fulfilment of requirements.

2) Convergence assurance in iterative proceedings, with little processing.

3) Versatility on requirements values setting, priority setting, and precision to be achieved, which may be refined with no practical impact on response time.

Studies on the subject continue, as on orbit transfer not necessarily by orbit perigee, and on controllable last stage.

## References

[1] Robbins, H. M. 1966. An analytical study of the impulsive approximation. AIAA Journal, v. 4, n. 8: 1417-1423.
[2] Bate, R. R., D. D. Mueller and J. E. White. 1971. Fundamentals of astrodynamics. Dover Publications.
[3] Leite Filho, W. C. and P. S. Pinto. 1998. Guidance strategy for solid propelled launchers. Journal of Guidance, Control and Dynamics, v. 21, n. 6: 1006-1009.
[4] Franklin, P. 1958. Marks mechanical engineer's handbook, chapter 2: Mathematics. McGraw-Hill.
[5] Wertz, J. R. 1978. Spacecraft attitude determination and control. Kluwer Academic Publishers.